Chapter 11

Boiling Heat Transfer Inside Enhanced Tubes

SUMMARY: In this chapter, evaporation inside enhanced tubes and in tubes with inserts is described. Both evaporation in vertical tubes and horizontal tubes is addressed. The types of enhancements discussed include microfin tubes, twisted tape inserts, corrugated tubes, and internally porous coated tubes. Other enhancements exist but are either not widely used anymore (aluminium star-inserts and internally high finned tubes, for example), are not appropriate for enhancing boiling heat transfer, or do not have very much published about their thermal performance. Several prediction methods are presented for microfin tubes and tubes with twisted tape inserts.

11.1 Introduction

In vertical tubes, the most important applications and potential benefits for use of enhancements for evaporation are in the petrochemical industry and hence for vertical thermosyphon reboilers. These units typically evaporate from 10% to 35% of the flow while the inlet is slightly subcooled from the static head with respect to the liquid level in the distillation tower. This application also implies that evaporation of zeotropic multi-component mixtures is of interest, for which little or no data are available in the literature for most enhancements for vertical upflow. Some representative results are presented below for enhanced heat transfer inside vertical tubes.

In horizontal tubes, the most important applications of enhancements are to direct-expansion evaporators in refrigeration, air-conditioning and heat pump units. In the petrochemical industry occasionally a horizontal, tube-side evaporator is used for a service but this is the exception rather than the rule. In direct-expansion evaporators, the fluid enters the tubes after the expansion valve and hence the range of interest is from about 15% to 100% vapor quality, in addition to the superheating zone. Instead, in recirculation type units often favored by ammonia system manufacturers, the fluid enters as a saturated liquid and about 20% to 30% of the fluid is evaporated at the exit. Most of this chapter focuses on microfin tubes, which are of highest industrial interest, while some other enhancement geometries will also be addressed.

The focus here is on more recent work, primarily that done since 1990. Refer to the book by Thome (1990) for a comprehensive treatment of studies done prior to 1990. Shatto and Peterson (1996) also wrote an extensive review on evaporation in tubes with twisted tapes, covering aspects such as the critical heat flux and dryout.

The standard practice for enhanced boiling inside tubes is to define the internal heat transfer coefficient based on the nominal area at the maximum internal diameter, i.e. at the root of the fins for microfin tubes or that of the plain tube surface for a twisted tape insert. Nearly all test data respect this norm, although not all and hence one must remember to look at this point when comparing data from different sources. For example, some data in the literature are reported based on a nominal diameter at the fin tips or at a mean height of internal fins. However, when calculating the overall heat transfer coefficient for a heat exchanger, that at the maximum internal diameter is required. Hence, the maximum internal diameter will be used here for the nominal diameter and the nominal area corresponding to this diameter will be used for defining heat transfer coefficients and heat fluxes, unless otherwise stated.

11.2 Types of Enhancements and Performance Ratios

The following enhancements are described here for evaporation: microfin tubes, twisted tape inserts, corrugated tubes and tubes with porous coatings. Microfin tubes are also sometimes referred to as inner-grooved tubes. Microfin tubes were originally developed in Japan and widespread use of microfin tubes began in the 1980's. Microfin tubes quickly overtook and replaced the use of star-insert tubes, i.e. tubes with star-shaped aluminum inserts tightly fit into copper tubes, which had been popular up until then. Twisted tape inserts and corrugated tubes have been commercially available for many years, although both have been largely supplanted by microfin tubes. Twisted tape inserts, even with their lower thermal performance and higher two-phase pressure drops, are still a viable alternative as they can be easily retrofit into existing plain-tube equipment without retubing. Corrugated tubes are also still used for a variety of applications.

Figure 11.1 depicts a photograph of the fin profile of a microfin tube. Figure 11.2 shows the characteristic geometry, which is defined by the maximum internal diameter d_f, number of fins, their helix angle α_f (or axial pitch), their height e_f, their thickness, their cross-sectional shape and the internal area ratio. Most microfins have approximately a trapezoidal cross-sectional shape with a rounded top and rounded corners at the root. Other shapes are triangular, rectangular and screw (no root area between fins). The thickness of the fins is not of much importance since the fin efficiencies are close to 1.0 even in alloy tubes since the fins are typically only from 0.2 to 0.3 mm (0.008-0.012 in.) high.

Figure 11.1. Photograph of fin profile of microfin tube of Wolverine Tube Inc.

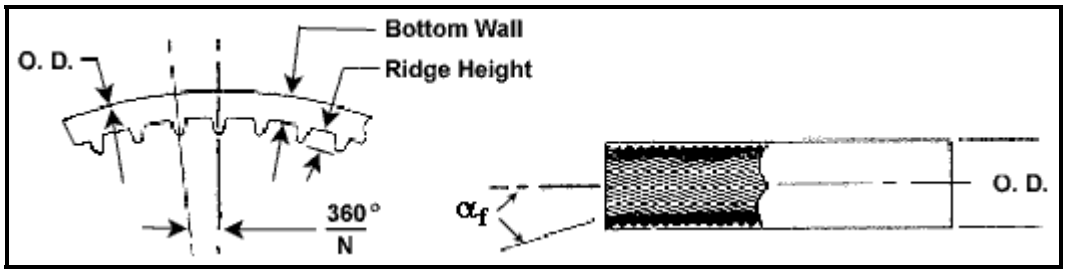

Figure 11.2. Microfin tube geometry of Wolverine Tube Inc.

Figure 11.3 depicts a photograph of a twisted tape insert and a diagram of its geometry. The twist ratio is defined as the axial length of tape necessary to make a 180° turn divided by the tube internal diameter. Twist ratios of 3 to 5 are typically used while a twist ratio of infinity represents a straight tape without any twist. As twisted tape inserts fit loosely inside the tubes, the surface area of the tape is not considered to be heat transfer surface area since little heat is conducted into the tape from the tube wall.

Figure 11.3. Photograph of twisted tape insert and diagram of its geometry.

Figure 11.4 illustrates a photograph of a corrugated tube and a diagram with its characteristic dimensions. Most corrugated tubes have a single-start of corrugation that is defined by its depth e and its axial pitch p (or helix angle). The maximum internal diameter is typically used to define the internal heat transfer coefficient. The internal area ratio is slightly larger than 1.0 but is not often cited in publications.

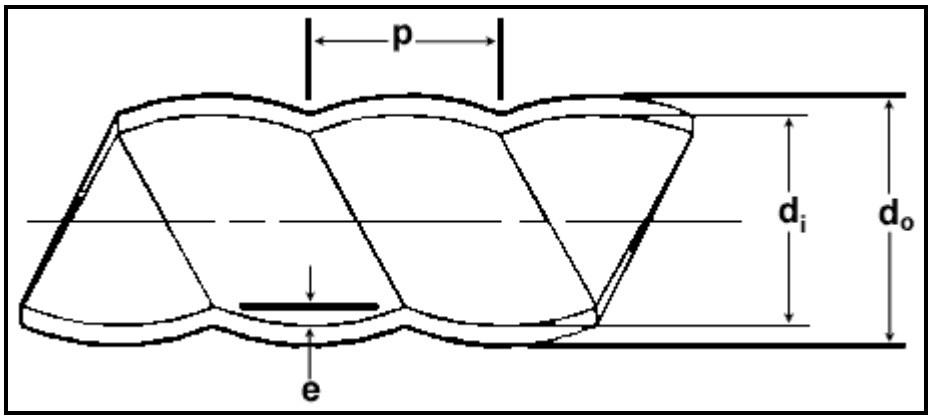

Figure 11.4. Photograph and diagram of Korodense corrugated tube of Wolverine Tube Inc.

Microfin tubes are available primarily in copper. For instance, Wolverine Tube Inc. is a major manufacturer of copper microfin tubes for the air-conditioning and refrigeration industries. Seamless microfin tubes are produced by drawing a plain copper tube over a mandrel to form helical fins. This production method allows microfins to be produced from about 0.1 to 0.4 mm (0.004 to 0.016 in.) in height. The most favorable helix angles for heat transfer and pressure drop range from about 7° to 23°, but 18° seems to be the most popular. Instead, welded microfin tubes are formed from copper strip, whose microfin geometry has been embossed by a rolling operation. This manufacturing method allows a much wider range of microfin geometries to be produced, including 3-dimension fin geometries. In addition, microfin tubes are also becoming available in other materials, such as aluminum, carbon steel, steel alloys, etc.

Corrugated tubes are manufactured in many metals: copper, copper alloys, carbon steels, stainless steels and titanium. The corrugations are defined by the corrugation pitch, corrugation depth and number of corrugations, i.e. the number of starts. Multi-start corrugated tubes with large corrugation depths are typically referred to as fluted tubes.

Twisted tape inserts are available in most metals, diameters and lengths. They are made by twisting metal strip and fit loosely in the tubes to allow for standard tube wall dimensional tolerances.

As an example of enhancement ratios achievable with these geometries, relative to a plain tube of the same diameter at the same mass flux and heat flux, some general qualitative guidelines are as follows:

- **Microfin tubes**. For horizontal applications, heat transfer enhancement ratios are as high as three to four times at low mass velocities while falling off towards their internal area ratio at high mass velocities. Pressure drop ratios most often range from about 1.0 at low mass velocities and up to about a maximum of about 1.5 at high mass velocities. Hence, microfins are very attractive from a heat transfer augmentation to pressure drop penalty point-of-view. For vertical applications, the heat transfer enhancement is less or similar to horizontal expectations, depending on the mass velocity. The small increase in the frictional pressure drop by the microfins in a vertical unit is typically negligible compared to the static head pressure drop in these units and thus plain tube design methods can be used directly.

- **Twisted tape inserts**. Heat transfer augmentation ratios are typically in the range from 1.2 to 1.5 while two-phase pressure drop ratios are often as high as 2.0 since the tape divides the flow channel into two smaller cross-sectional areas with smaller hydraulic diameters. Twisted tapes have seen some applications in both horizontal and vertical units.

- **Corrugated tubes**. Heat transfer ratios are usually between 1.2 to 1.8 with performances matching microfin tubes at high mass velocities but with much larger two-phase pressure drop ratios, which are on the order of 2 times those of a plain tube. Apparently, little experience is available for vertical applications.

- **Porous coated tubes**. These have heat transfer performances similar to those for nucleate pool boiling and are on the order of 5 to 10 times plain tube performance in vertical tubes. For evaporation in horizontal tubes, the porous coating is only effective for annular flows but not for stratified flows where part of the tube perimeter is dry. Not much information is available about two-phase pressure drop penalties, which can be expected to be only marginal in vertical units where the static head dominates while significant in horizontal tubes where the frictional pressure drop is typically dominant.

11.3 Flow Boiling in Vertical Microfin Tubes

For microfin tubes, apparently only one test has been done for evaporation in the vertical orientation. Kattan, Thome and Favrat (1995) ran tests for R-134a in a microfin tube with an 11.90 mm (0.469 in.) maximum internal diameter, 18° helix angle, 0.25 mm (0.010 in.) fin height and 60 fins for an internal area ratio of 1.74. Hot water was used as the heating source and the modified-Wilson plot method applied to three zones of a 3 m (10 ft.) long tube to obtain quasi-local heat transfer data. They ran tests for the same test section for vertical upflow and horizontal flow under identical operating conditions to determine the possible benefit of using microfins in vertical thermosyphon reboilers. At low mass velocities and vapor qualities, there was less augmentation in the vertical position than in the horizontal position relative to a plain tube because a vertical plain tube does not suffer from the adverse effect of flow stratification like a horizontal plain tube. On the other hand, at higher mass velocities the level of augmentation was similar and at least as large or larger than the increase in surface area. Figure 11.5 for instance compares their horizontal and vertical flow boiling data for the microfin tube at a mass velocity of 201.2 kg/m^{2}s (148000 lb/hr ft^2) at 4.2 bar (60.9 psia), which is a typical flow rate for vertical thermosyphon operation. The performance in the vertical orientation is slightly less than that of the microfin tube compared its horizontal orientation over the range of vapor qualities from 0.23 to 0.5. Heat transfer augmentation is on the order of 2 or more for all the data.

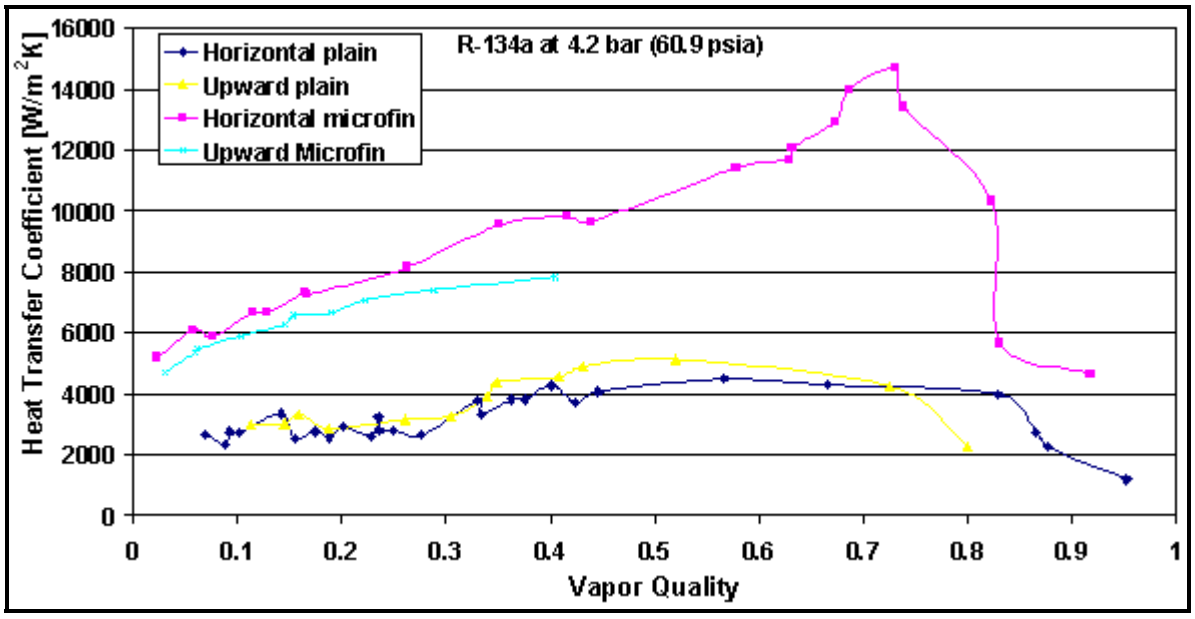

Figure 11.5. Effect of tube orientation on evaporation in a microfin tube from Kattan, Thome and Favrat (1995b) at 201.2 kg/m^{2}s (148000 lb/hr ft^2).

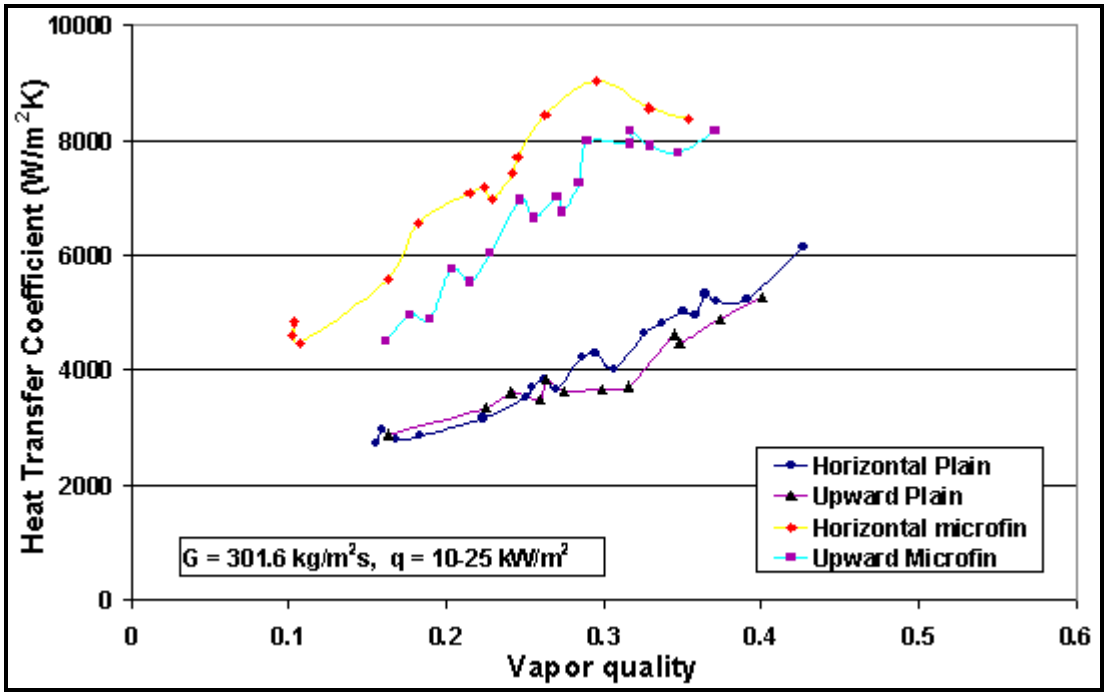

Figure 11.6. Effect of tube orientation on evaporation in a microfin tube from Kattan, Thome and Favrat (1995b) at 301.6 kg/m^{2}s (222000 lb/hr ft^2).

Figure 11.6 shows more R-134a data for the same microfin tube at a mass velocity of 301.6 kg/m^{2}s (222000 lb/hr ft^2) at the same pressure. Here, the performance in the vertical microfin tube is less than that of the horizontal microfin tube for vapor qualities from 0.16 to 0.37. Heat transfer augmentation is still on the order of 2. Notably, when replacing a vertical plain tube bundle with a vertical microfin tube

bundle, the number of tubes required is less and the microfin tube bundle benefits for the above augmentation ratio in addition to a higher mass velocity, heat flux and exit vapor quality, which further improve the heat transfer performance by perhaps another 50%.

11.4 Flow Boiling in Vertical Tubes with Twisted Tape Inserts

Twisted tape inserts have the distinct advantage in that they can be used to increase the thermal capacity of existing evaporators without replacing the tube bundle. Twisted tapes fit loosely within the tubes and hence they enhance heat transfer by the swirl that they impart on the flow but do not provide any additional heat transfer surface area.

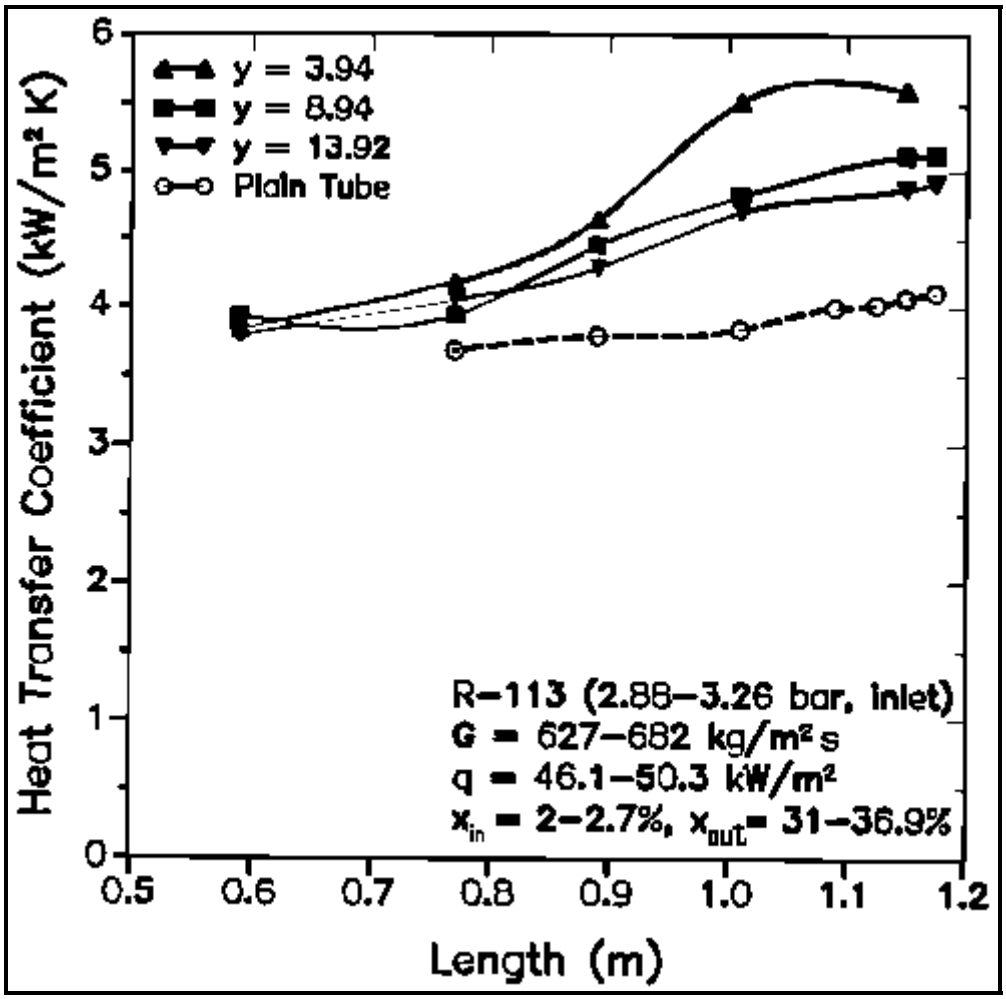

Figure 11.7. Effect of twist ratio on evaporation of R-113 from Jensen and Bensler (1986).

Most experimental tests with twisted tape inserts have been performed for evaporation in horizontal tubes. Jensen and Bensler (1986) studied the effect of twist ratio, y, defined here as the ratio of the axial length for a 180° twist of the tape to the internal diameter of the tube, on boiling of R-113 in vertical upflow in a tube of 8.10 mm (0.319 in.) internal diameter using electrical heating. Figure 11.7 depicts a comparison between tubes with twisted tapes and one without, plotted as a function of position along the tube rather than vapor quality, where the vapor quality ranged from 0.02-0.027 at the inlet to 0.31-0.37 at the outlet.

The heat transfer coefficients and heat fluxes were calculated based on the internal surface area of the tube after subtracting the heat generated in the tapes themselves. Most of the augmentation is observed at the higher vapor qualities, where it is as much as 40%, while at low vapor qualities it is only on the order of 10%. These test conditions are not necessary indicative of the augmentation that could be attained in a vertical thermosyphon reboiler, for example, since the mass velocity and heat flux in these tests were quite high compared to typical operating conditions. The swirl effect would be expected to be more effective at lower mass velocities and lower heat flux where the potential for augmenting the convective contribution to the two-phase flow boiling coefficient is most evident.

11.5 Flow Boiling in Vertical Tubes with an Internal Porous Coating

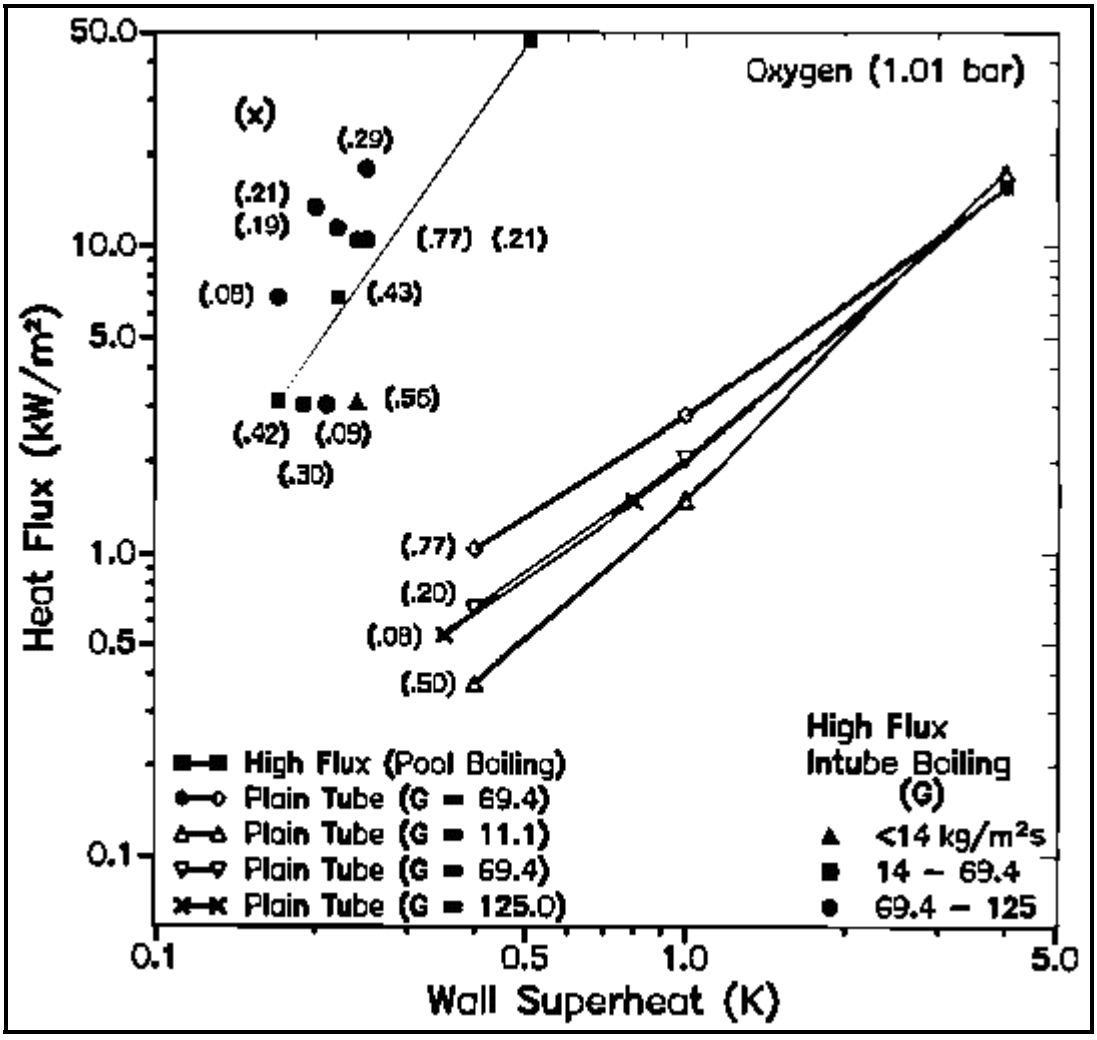

Figure 11.8. Evaporation of oxygen inside vertical High Flux tube relative to plain tube.

Applying a thin porous coating to the inside of vertical evaporator heat transfer tubes is very successful in improving performance. The commercially available enhanced tube High Flux (property and trademark first of Union Carbide and now of UOP) is available with the coating either inside or outside. As an

example of boiling performance, Figure 11.8 depicts intube boiling data for liquid oxygen in a 18.7 mm (0.736 in.) internal diameter High Flux tube, apparently obtained at 1.01 bar (14.7 psia), by Czikk, O'Neill and Gottzmann (1981). The local boiling heat transfer coefficients are plotted as heat flux versus wall superheat as would be typical of nucleate pool boiling since the High Flux heat transfer data are dependent on heat flux but are virtually independent of vapor quality and mass velocity. Comparable plain tube heat transfer coefficients predicted with the Chen (1963) correlation are also shown at similar conditions. In addition, the High Flux pool boiling curve obtained by Antonelli and O'Neill (1981) for liquid oxygen is also shown, which matches the flow boiling data remarkably well. Heat transfer augmentation is on the order of 10-fold. They have noted that single-tube nucleate pool boiling heat transfer data are suitable for predicting the flow boiling performance of the High Flux tube since the nucleate boiling contribution dominates the convective boiling contribution. Hence, their pool boiling curves for the High Flux tube can be used for the design of vertical thermosyphon reboilers for the same fluid.

11.6 Flow Boiling of Pure Fluids in Enhanced Horizontal Tubes

Below, a summary of experimental research published since 1990 on intube evaporation of pure refrigerants (and azeotropic refrigerant mixtures) inside horizontal enhanced tubes is presented. Selected studies are shown in Table 11.1 listing the test conditions, type of tube and dimensions as follows:

- $\dot{m}$ *(kg/m^{2}s)*: the mass velocity based on maximum internal diameter at the root of internal fins or corrugations.
- T_{sat} *or* P_{sat}: the saturation temperature or pressure of the tests.
- *Max ID*: the internal diameter at the root of any internal fins or corrugations.
- *No./Angle/Ht./AR*: the dimensions of the internal fins citing Number of fins/Helix Angle/Fin Height (mm)/Area Ratio (relative to nominal area at Max ID) or the characteristic dimensions of other types of tubes (fluted, twisted tape, helical wires, etc.).
- *Tube Type*: Microfin* with an asterisk refers crosscut microfins, i.e. notched 3-dimensional microfins.

Table 11.1. Evaporation Tests on Pure Refrigerants and Azeotropes in Enhanced Tubes

Reference	Test Conditions			Tube Description (in mm)		
Name (year)	**Fluid**	**$\dot{m}$(kg/m^{2}s)**	**T_{sat} or p_{sat}**	**Max ID**	**Type**	**No./Angle/Ht./AR**
Eckels-Pate (1991a)	R-134a	125-400	5, 10, 15°C	8.72	Microfin	60/17°/0.20/1.5
	"	"	5, 10, 15°C	8.00	Smooth	-
	R-12	"		8.72	Microfin	60/17°/0.20/1.5
	"	"		8.00	Smooth	-
Torikoshi et al. (1992)	R-134a	45-200	5, 15, 30°C	8.7	Smooth	-
		"		8.8	Microfin	60/18°/0.20/1.?
Hinton et al. (1992)	R-22	176-343	Not cited	16.8	Fluted	2-start, 0.8/7.1
		211-421	Not cited	13.85	Smooth	-
Eckels et al. (1992)	R-22	150-350	2, 7°C	9.52OD	MicrofinA	?/18°/0.18/1.?
	"	"	"	"	MicrofinB	?/18°/0.20/1.?
	"	"	"	"	MicrofinC	?/18°/0.20/1.?
	"	"	"	"	MicrofinD	?/18°/0.18/1.?
	"	"	"	"	MicrofinE	?/18°/0.18/1.?

Reference	Test Conditions			Tube Description (in mm)		
Name (year)	**Fluid**	**$\dot{m}$(kg/m^{2}s)**	**T_{sat} or p_{sat}**	**Max ID**	**Type**	**No./Angle/Ht./AR**
	R-22	135-400	2, 7°C	7.94OD	MicrofinC	?/18°/0.20/1.?
	"	"	"	"	MicrofinD	?/18°/0.18/1.?
	"	"	"	"	MicrofinE	?/18°/0.18/1.?
Christoffersen et al. (1993)	R-22	204-510	5°C	7.75	Smooth	-
	R-134a	102-510	"	"	"	-
	R-22	204-306	5°C	10.92	Smooth	-
	R-134a	102-510	"	"	"	-
	R-22	51-510	5°C	8.89	Microfin	60/18°/0.18/1.?
	R-134a	51-510	"	"	"	
Eckels et al. (1994)	R-134a	85-375	1°C	8.0	Smooth	-
	"	"	"	8.92	Microfin	60/17°/0.20/1.5
Torikoshi-Ebisu (1994)	R-22	85-520	5°C	6.40	Microfin	50/18°/0.18/1.?
Thors-Bogart (1994)	R-22	75-390	1.67°C	14.86	Smooth	-
	"	"	"	14.86	Microfin	60/27°/0.305/1.?
	"	"	"	14.86	Microfin	75/23°/0.305/1.?
	"	"	"	14.10	Corrugat.	1/78°/1.041/1.?
	R-22	125-430	1.67°C	8.72	Plain	-
	"	"	"	8.87	Microfin	60/18°/0.203/1.?
	"	"	"	8.87	Microfin	72/0°/0.203/1.?
Chamra-Webb (1995)	R-22	151-327	24.4°C	14.66	Microfin	74/15°/0.35/1.? (Crossgrooves)
Kuo et al. (1995)	R-22	100, 200	2, 6, 10°C	6.50	Microfin	60/18°/0.15/1.49
Kido et al. (1995)	R-22	86-345	4.9 bar	6.40	Smooth	-
	R-22	86-345	"	6.47	Microfin	60/18°/0.15/1.63
	"	173	"	6.50	"	70/11°/0.21/2.21
	"	173	"	6.55	"	70/17°/0.21/2.24
	"	86, 173	"	6.52	"	85/ 9°/0.16/2.07
	"	86, 173"	"	6.54	"	85/17°/0.16/2.13
	"	173	"	6.48	"	85/ 7°/0.21/2.49
	"	-	"	6.56	"	100/3°/0.15/2.19
Kattan et al. (1995b)	R-134	100-300	2.8-4.2 1.07	11.90	Microfin	70/18°/0.25/1.74
	R-123	100-300	bar	11.90	Microfin	70/18°/0.25/1.74
Koyama et al. (1996)	R-134a	307	6.55 bar	8.475	Microfin	60/18°/0.17/1.52
MacBain-Bergles (1996)	R-12	100-400	3.20 bar	12.5	Fluted	3-start/2.7/7.94
Wang et al. (1996), Kuo-Wang (1996a, 1996b)	R-22	100-300	6 bar	7.92	Smooth	-
	R-22	100-300	6 bar	8.92	Microfin	60/18°/0.20/1.57
Singh et al. (1996)	R-134a	50-150	5.75 bar	11.78	Microfin	60/18°/0.30/1.?
Chamra et al. (1996)	R-22	45-181	2.2°C	14.86	Smooth	-
	R-22	45-181	2.2°C	14.88	Microfin	74/27°/0.35/1.?
	"	"	"	"	"	78/20°/0.35/1.?
	"	"	"	"	"	76/17.5°/0.35/1.?
	"	"	"	"	"	80/15°/0.35/1.?
	"	"	"	"	Microfin*	74/27°/0.35/1.?
	R-22	45-181	2.2°C	14.88	Microfin*	78/20°/0.35/1.?
	"	"	"	"	"	76/17.5°/0.35/1.?

Reference	Test Conditions			Tube Description (in mm)		
Name (year)	**Fluid**	**$\dot{m}$(kg/m^{2}s)**	**T_{sat} or p_{sat}**	**Max ID**	**Type**	**No./Angle/Ht./AR**
	"	"	"	"	"	80/15°/0.35/1.?
Kaul et al. (1996)	R-22	314, 364	4.4°C	8.93	Mcrofin	?/?/?/1.?
	R-32	"	"	"	"	"
	R-125	"	"	"	"	"
	R-134a	"	"	"	"	"
Nidegger et al.(1997)	R-134a	100-300	4.4°C	11.90	Microfin	70/18°/0.25/1.74
Zürcher et al. (1997b)	Ammo-	20-120	4°C	14.00	Smooth	-
	nia	"	"	13.46	Microfin	34/18°/0.33/1.33
MacBain et al. (1997)	R-12	100-400	3.20 bar	12.5	Fluted	3-start/2.7/7.94
	R-134a	"	"	"	"	"
Kedzierski-Kim (1997)	R-12	Not cited	Reduced	9.64	Twisted	y=4.15
	R-22	"	Press. from	"	Tape	"
	R-152a	"	0.035-0.2	"	"	"
	R-134a	"	"	"	"	"
	R-290	"	"	"	"	"
	R-290/	"		"	"	"
	R-134a		"			
	R-134a/	"		"	"	"
	R-600a					
Lan et al. (1997a)	R-113	514-2972	7.9 bar	6.2	Helical	0.81 dia. wire
	"	"	"	"	Wire	"
Lan et al. (1997b)	R-113	305-4361	7.9 bar	6.2	Helical	0.81 dia. wire
	"	"	"	"	Wire	"
Muzzio et al. (1998)	R-22	90-400	5°C	8.92	Smooth	-
	R-22	90-400	5°C	8.92	Microfin	54/18°/0.16-0.23/1.51
	"	"	"	8.92	"	60/18°/0.20/1.51
	"	"	"	8.84	"	65/25°/0.15/1.28
Oh-Bergles (1998)	R-134°	50-200	3.1 bar	8.21	Smooth	-
	"	"	"	8.71	Microfin	60/6°/?/?
	"	"	"	"	"	60/12°/?/?
	"	"	"	"	"	60/18°/?/?
	"	"	"	"	"	60/25°/?/?
	"	"	"	"	"	60/44°/?/?
Kabelac-de Buhr	Ammo-	50-150	-20°, 4°C	10.0	Smooth	-
(2001)	nia	50-150	-20°C	11.13	Microfin	21/25°/0.63/1.58
Lallemand et al. (2001)	R-22	150-250	7.7 bar	10.7	Smooth	-
	"	"	"	11.98	Microfin	65/30°/0.25/1.56
	"	"	"	11.98	Microfin	70/20°/0.22-0.25/1.69

A few of the investigations listed in Table 11.1 are described below.

Eckels and Pate (1991a) investigated evaporation in a single microfin tube for refrigerants R-134a and R-12, in a continuation of their earlier study on a plain tube presented in Eckels and Pate (1991b). They reported mean heat transfer coefficients for a vapor quality change of about 75% from inlet to outlet of their test section using counter-current hot water flow. They found slightly smaller microfin enhancement

ratios for R-134a than for R-12. The augmentation ratios were higher at low mass velocities (2.3 to 2.6 times the plain tube coefficients) than at higher mass velocities (1.7 to 1.9 times), compared to the tube's area ratio of 1.5, which was typical of prior studies by others for R-22.

An extensive experimental program by Thors and Bogart (1994) covered two sizes of tubes, 3/8 in. (9.5 mm) and 5/8 in. (15.88 mm), for plain, microfin and corrugated tubes using counter-current hot water heating in 3.66 m (12 ft.) long test sections. Their mean flow boiling coefficients were for an inlet vapor quality of 0.10 and an outlet vapor quality of 0.80 at a saturation temperature of 1.67°C (35°F). Figure 11.9 depicts their results for the 5/8 in. tubes (refer to Table 11.1 for the enhancement dimensions). Heat transfer augmentation for the 75-fin microfin tube was the highest, whose enhancement ratio was nearly four. At very high mass velocities, the corrugated tube's performance nearly matched that of the two microfin tubes, but at a much larger pressure drop penalty. [Refer to the chapter on two-phase pressure drops for their test data with these tubes].

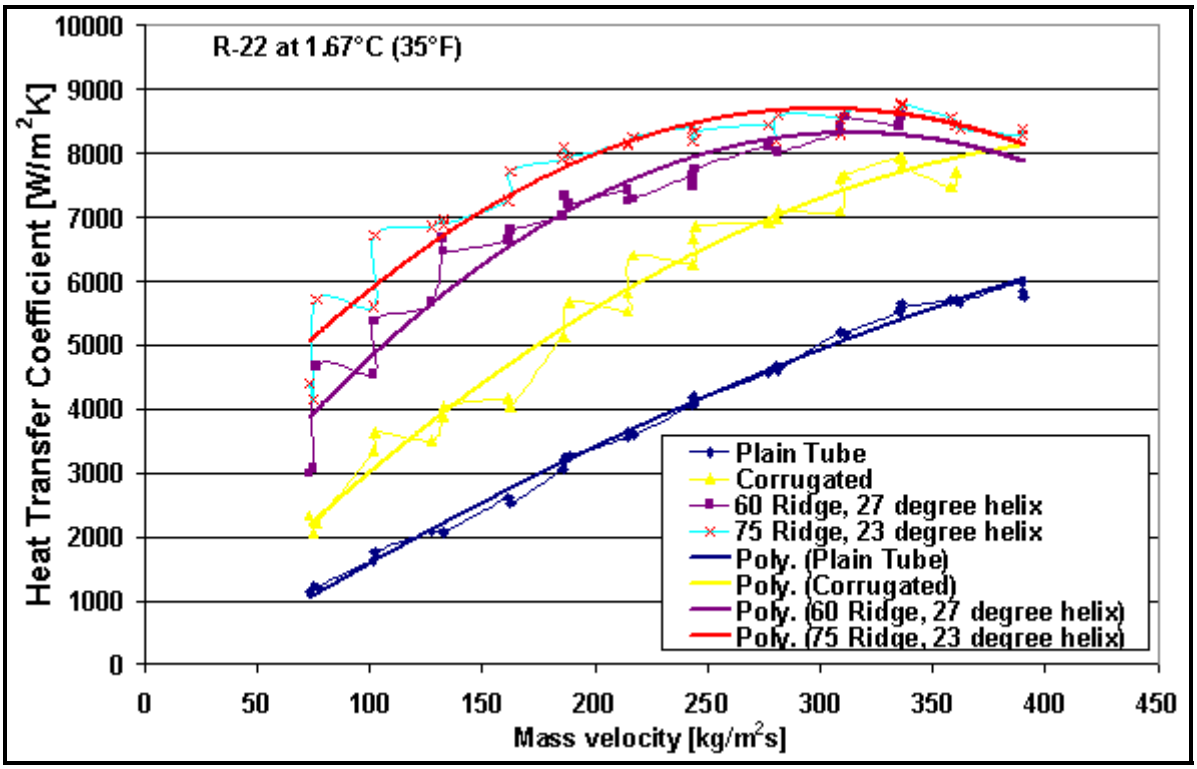

Figure 11.9. Flow boiling of microfin, corrugated and plain tubes by Thors and Bogart (1994) for R-22.

Chamra and Webb (1995) measured quasi-local heat transfer coefficients for R-22 using hot water heating. Their microfin tube had fins with a 15° helix angle, which were crosscut to make three-dimensional fins. Interestingly, they measured both flow boiling and condensation heat transfer data at similar test conditions, illustrating that in annular flow the heat transfer processes for evaporation and condensation give similar heat transfer coefficients, except for the additional effect of nucleate boiling. They observed mean augmentation levels up to 3.5 at low mass velocities in the range of 50 kg/m^{2}s (36,791 lb/hr ft^2) that decreased to 1.7 at 200 kg/m^{2}s (147,162 lb/hr ft^2).

A comparative study for local flow boiling coefficients between a microfin tube and a plain tube for R-134a was made by Nidegger, Thome and Favrat (1997) and Zürcher, Thome and Favrat (1997a) at 4.4°C (40°F) using counter-current hot water for heating. The two test sections in series, each 3 m (10 ft.) long,

were divided into three subsections of 1 m (3.28 ft) length each, and thus gave quasi-local heat transfer data of each subsection. Augmentation was observed over the entire range of vapor qualities. [Note: some of their data are shown later in a comparison to R-407C in Figure 11.12].

Zürcher, Thome and Favrat (1997b) obtained data for evaporation of ammonia in a stainless steel plain tube and a stainless steel microfin tube, both made in 439-grade steel. The tubes in their test sections were tightly wrapped with a helical wire that was fixed by spot soldering, thus increasing the water-side heat transfer coefficient by about 2 times. Four thermocouples were installed around the circumference of each tube to determine the mean tube wall temperature at two axial locations. They also measured the water temperature profile using thermocouples located along the hot water annulus, determined the local enthalpy gradient on the water-side, then the local heat fluxes to test locations, and thus obtained local boiling heat transfer coefficients rather that quasi-local values. Figure 11.10 depicts their results at four mass velocities. The microfins enhanced local heat transfer coefficients by about 2.2 times at low vapor qualities and up to 7.7 times at high vapor qualities while mean enhancement ratios were 4 to 5 for mass velocities less than 80 kg/m^{2}s (58,865 lb/hr ft^2) compared to the tube's area ratio of 1.33. At larger mass velocities, no enhancement was evident. At very low mass velocities, the enhancement ratio began to diminish, most likely because the flow remained stratified in the bottom of the tube.

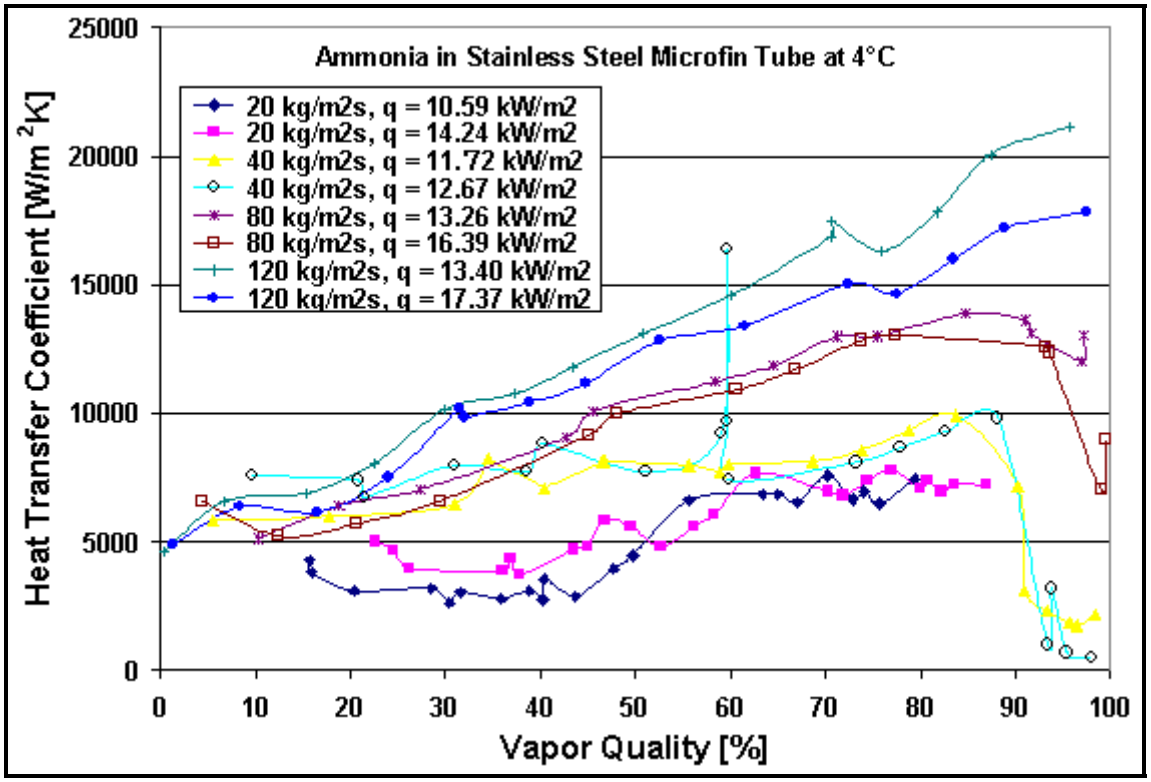

Figure 11.10. Zürcher, Thome and Favrat [1997b] ammonia flow boiling data for a microfin tube at 4°C (40°F).

Muzzio, Niro and Arosio (1998) measured heat transfer and pressure drops for four tubes for R-22: a plain tube, a microfin tube with alternating fins of 0.23 mm and 0.16 mm (0.009 and 0.006 in.) height, a second microfin with a conventional microfin geometry, and a third microfin with a *screw* profile. Quasi-local heat transfer coefficients were measured with a vapor quality change of 30% in their test sextion. The duo-height microfin tube gave significantly higher heat transfer performance than the other two tubes without much additional presssure drop penalty.

In a comparative study on the effect of microfin helix angle, Oh and Bergles (1998) investigated evaporation of R-134a in similar 60-fin microfin tubes with helix angles of 6°, 12°, 18°, 25° and 44°, although not mentioning the fin height nor the area ratios. They found the optimal helix angle at a vapor quality of 0.5 to depend on mass velocity, with the angles of 6° to 18° giving the best enhancement ratios.

Kabelac and de Buhr (2001) compared flow boiling of ammonia inside a 10.0 mm (0.394 in.) ID plain tube to an 11.13 mm (0.438 in.) ID microfin tube, both made in aluminum. They condensed ammonia on the outside of the tubes and accounted for axial heat conduction from the resulting temperature gradient. Their smooth tube data at 4°C compared well with those of Zürcher, Thome and Favrat (1999) for a slightly larger 14.0 mm (0.551 in.) stainless steel tube and showed that the Kattan, Thome and Favrat (1998a, 1998b, 1998c) plain tube heat transfer model predicted most of their data quite well. They also obtained local boiling coefficients for mass velocities of 50, 100 and 150 kg/m^{2}s at –20°C. The enhancement ratios were from about 1.7 to 4.3, compared to the tube's area ratio of 1.58. The data were taken primarily at low vapor qualities, particularly useful for ammonia refrigeration system evaporators operating with liquid recirculation.

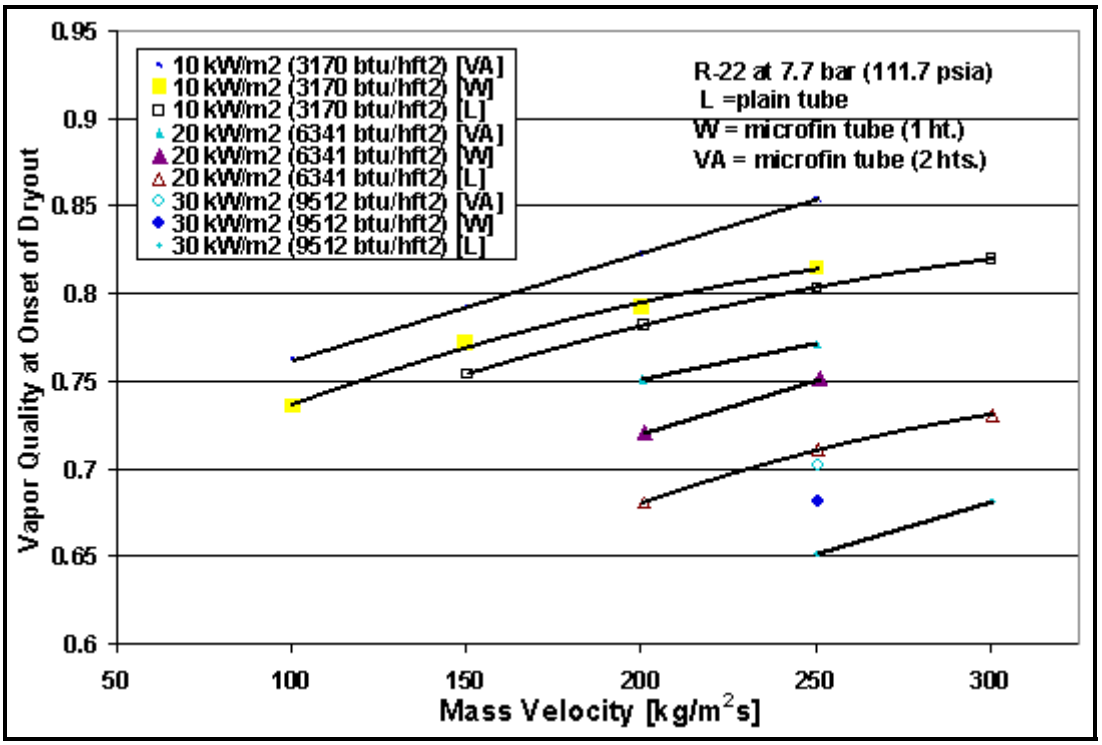

Figure 11.11. Influence of mass velocity on the onset of dryout for R-22 in a plain tube and two microfin tubes by Lallemand, Branescu and Haberschill (2001).

An interesting study on evaporation of R-22 (and R-407C) in a 10.7 mm (0.421 in.) plain tube and two 11.98 mm (0.472 in.) microfin tubes at a saturation pressure of 7.7 bar (111.7 psia) was done by Lallemand, Branescu and Haberschill (2001) for vapor qualities from 0.08 to 1.0 but using electrical heating. Their second microfin had microfins of alternating heights of 0.22 and 0.25 mm (0.009 and 0.010 in.), identified as tube VA. Significantly, they measured numerous data at high vapor qualities around the peak in the local heat transfer coefficient vs. vapor quality that occurs in annular flow at the onset of dryout at the top of the tube in horizontal tubes. Figure 11.11 shows their graph for the vapor quality at the onset of dryout plotted versus mass velocity for the three tubes, ranging from 0.65 to 0.85 depending

on the heat flux and mass velocity. The trends in these data match those predicted by the diabatic flow pattern map of Kattan, Thome and Favrat (1998a) for plain tubes with quite similar values for onset of dryout (my personal comparison). The microfins shifted the onset of dryout to slightly higher vapor qualities compared to their plain tube observations, but not significantly so.

11.7 Flow Boiling of Zeotropic Mixtures in Enhanced Horizontal Tubes

Before proceeding, some comments on the reduction of test data obtained in evaporation tests on zeotropic mixtures to heat transfer coefficients are in order. For the evaporation of a pure refrigerant, the enthalpy change and local vapor quality can be obtained using only the latent heat of the fluid and its mass flow rate, assuming the pressure drop is small, and the local saturation temperature can be obtained from the local saturation pressure. For a zeotropic mixture, the enthalpy change includes both differential latent heat of evaporation *and* the sensible heat added to the vapor and liquid phases along the bubble point curve of the mixture. Thus, the enthalpy curve of the mixture must be applied and used to calculate the local vapor quality and local bubble point temperature T_{bub}, where the local mixture boiling coefficient is defined as $\alpha = q/(T_{wall}-T_{bub})$. The bubble point temperature rises along the test section as the lighter component preferentially evaporates out of the liquid phase into the vapor phase. Hence, its value must be determined step-wise along the test section channel using an accurate vapor-liquid equilibrium prediction method. Numerous zeotropic refrigerant heat transfer data have unfortunately made it into the literature without use of such an enthalpy curve and thus one must always control this point before using such data.

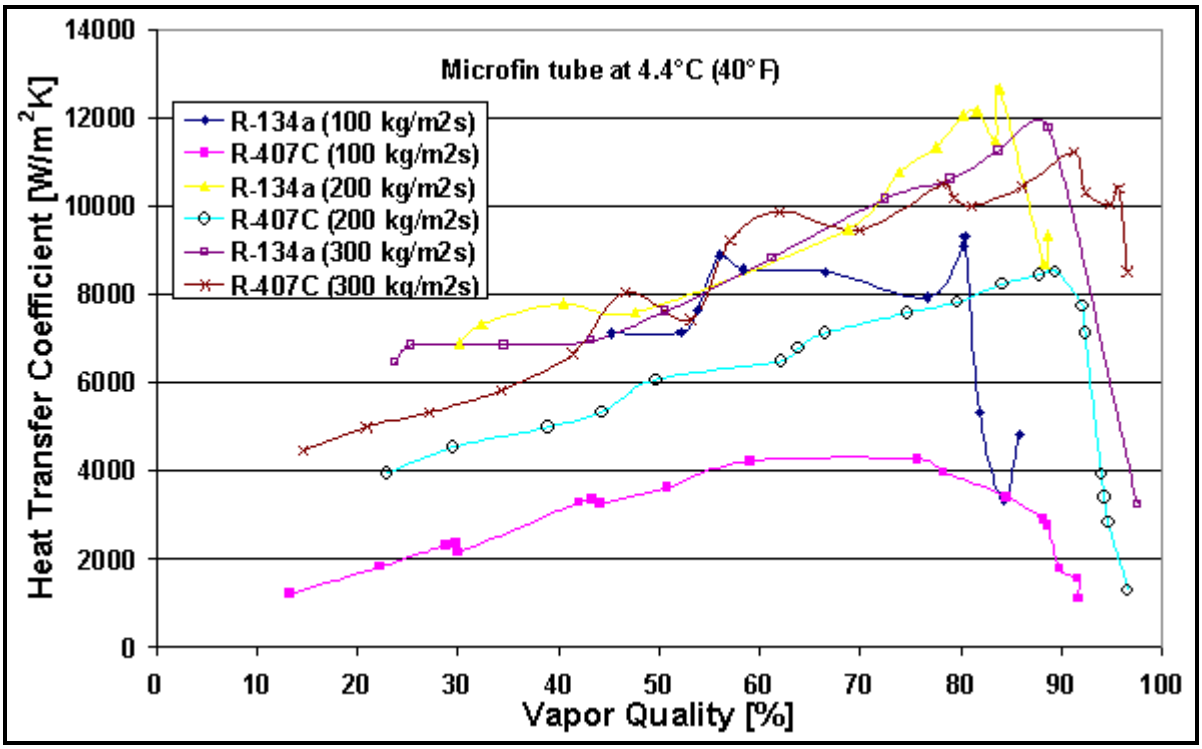

Figure 11.12. Zürcher, Thome and Favrat (1998a, 1998b) data comparing R-407C to R-134a in microfin tube.

Selected studies since 1990 on evaporation of zeotropic refrigerant mixtures inside enhanced tubes are listed in Table 11.2, most of which have used an enthalpy curve to reduce test data. A few of those are described below.

Table 11.2. Evaporation Tests on Zeotropic Refrigerant Mixtures in Enhanced Tubes

Reference	Test Conditions			Tube Description (mm)		
Name(year)	**Fluid**	**$\dot{m}$(kg/m^{2}s)**	**T_{sat} or P_{sat}**	**Max ID**	**Type**	**No./Angle/Ht./AR**
Christoffersen et al. (1993)	R-32/ R-125	204-510	5°C	7.75	Smooth	-
	"	204-510	5°C	10.92	Smooth	-
	"	51-510	5°C	8.89	Microfin	60/18°/0.18/1.?
Torikoshi-Ebisu (1994)	R-32/ R-134a	130-500	5°C	6.40	Microfin	50/18°/0.18/1.?
	"	"	"	"	"	"
	R-32/ R-125/ R-134a	130-510	"	"	"	"
Wang et al. (1996), Kuo-Wang [1996a, 1996b)	R-407C	100-300	6 bar	7.92	Smooth	-
	R-407C	100-300	6 bar	8.92	Microfin	60/18°/0.20/1.57
Sundaresan et al. (1996)	R-407C	125-375	7°C	8.0	Smooth	-
	"	"	"	8.72	Microfin	60/17°/0.20/1.5
	R-410A	125-375	7°C	8.0	Smooth	-
	"	"		8.72	Microfin	60/17°/0.20/1.5
Salehi et al. (1996)	R-404A	50-200	11.0 bar	11.78	Microfin	60/18°/0.25/1.?
Kaul et al. (1996)	R-410B	314, 364	4.4°C	8.93	Microfin	?/?/?/1.?
	R-407C	314, 364	4.4°C	"	"	"
	R-32/ R-125	314, 364	4.4°C	"	"	"
Kedzierski-Kim (1997)	R-32/ R-134a	Not cited	Reduced Press.	9.64	Twisted Tape	y=4.15
	R-32/ R-152a	"	0.035-0.2	"	"	"
Zürcher et al. (1998a,1998b)	R-407C	100-300	4.4°C	10.92	Smooth	-
	"	"	"	11.90	Microfin	70/18°/0.25/1.74
Ebisu-Torikohi (1998)	R-407C	150-300	5.5 bar	6.5	Microfin	Herringbone
Cho-Kim (1998)	R-407C	200, 400	6.5 bar	8.82	Smooth	-
	R-407C	200, 400	6.5 bar	8.53	Microfin	?/18°/?/?
Lallemand et al. (2001)	R-407C	150-250	7.7 bar	10.7	Smooth	-
	"	"	"	11.98	Microfin	65/30°/0.25/1.56
	"	"	"	11.98	Microfin	70/20°/0.22-25/1.69

Flow boiling tests for R-407C evaporating in a plain tube and a microfin tube were performed by Zürcher, Thome and Favrat (1998a, 1998b) using hot water heating. They specifically obtained data at high vapor qualities before and after the peak in α_{tp} vs. x. Their test data for the microfin tube at an inlet boiling point

temperature of 4°C (40°F) are shown in Figure 11.12, in a comparison of R-407C to R-134a. While their 300 kg/m^{2}s (220,743 lb/hr ft^2) data were similar to R-134a (note: R-134a is a pure fluid and is one of the components in R-407C), the R-407C data were much lower than those of R-134a at the lower two mass velocities. It is not clear why, except for the increased mass transfer resistance at the lower flow rates.

Ebisu and Torikoshi (1998) presented results for R-407C evaporating in a herringbone type of microfin tube. Curiously, their heat transfer coefficients were based on the outside tube diameter rather than the internal diameter. From their circumferential temperature measurements around the perimeter of the tube, they deduced that the herringbone structure created a thicker liquid film at the top and bottom of the tube and thinner films at the two sides. The heat transfer coefficients were 90% higher than for a comparable helically finned microfin tube, but the herryingbone geometry had a higher pressure drop. Cho and Kim (1998) reported heat transfer measurements around a U-bend of a microfin tube, whose fin dimensions were not mentioned. The U-bend increased heat transfer in the bend and for a short length after the bend by 4 to 33%.

11.8 Flow Boiling Models for Horizontal Microfin Tubes

The first boiling model developed for microfin tubes was that of Thome (1991) that became available in an enhanced heat transfer software program in 1991. A completely general method for microfin geometries was formulated that covered helix angles from 0° to 30°, a number of microfins up to 80, fin heights up to 0.6 mm (0.024 in.) and included the effects of mass velocity and internal surface area ratio. It was originally based on test data for pure refrigerants R-11, R-12, R-113 and R-22 available at that time for numerous microfin tube geometries and tube diameters up to 5/8 in. (15.9 mm). It has since been successfully compared against more recent data for new refrigerants, such as R-134a and R-123, new data for ammonia and zeotropic refrigerant mixtures, such as R-407C.

Table 11.3. Simulations for R-134a at 200 kg/m2 s (147000 lb/hr ft2) at 3°C (5.4°F)

Tube	Plain	Microfin #1	Microfin #2	Microfin #3
O.D. (mm)	9.525	9.525	9.525	9.525
I.D. (mm)	8.509	8.509	8.509	8.509
Number of Fins	NA	21	60	75
Fin Height (mm)	NA	0.38	0.20	0.20
Spiral Angle (°)	NA	30	18	18
Area/L (m^2/m)	0.0267	0.0481	0.0411	0.0438
I.D. Area Ratio	1.0	1.8	1.5	1.6
α_{boil} (W/m^2 K)	2741	4951	5649	5917
α_{sup}(W/m^2 K)	392	795	663	694
Δp (kPa)	25.61	55.44	29.22	29.32
EF_{boil}	1.0	1.806	2.061	2.159
EF_{sup}	1.0	2.028	1.691	1.770
EF_p	1.0	2.165	1.141	1.145

A parametric study was presented using this method in Thome (1994a) for R-134a for a plain tube, a tube with a twisted tape insert, and three microfin tube geometries. The results are shown in Table 11.3. The microfin tube geometries listed are based on two commercial tubes available at that time (#1 and #2) and a hypothetical tube (#3). All tubes had an external diameter of 9.52 mm (3/8 in.) and a wall thickness of 0.508 mm (0.02 in.), giving an internal diameter of 8.51 mm (0.335 in.). A plain tube and a plain tube with twisted tape, 0.5 mm (0.02 in.) with a twist ratio of four, were also simulated for comparison

purposes. All tubes were assumed to have a length of 6.0 m (19.7 ft.), an inlet vapor quality of 0.15 and 5°C (9°F) of superheating at the outlet. A mass velocity of 200 kg/m^{2}s (147,000 lb/hr ft^2) and a nominal internal heat flux of 8105 W/m^2 (2570 Btu/h ft^2) were simulated. The boiling zone heat transfer coefficients are mean values from local calculations over the vapor qualities from 0.15 to 1.0 while the superheated coefficients are for single-phase superheating of the vapor. The pressure drops are the total pressure drops for both the evaporating and superheating zones. The enhancement factors (EF) are the respective heat transfer and pressure drops relative to the plain tube. The parametric study shows that the twisted tape is much less effective than the microfin tubes while having a larger pressure drop. The microfin tubes augment heat transfer substantially in both the boiling and superheated zones.

Fujii et al. (1993) next proposed the following microfin correlation:

$$Nu_{mf} = \frac{\alpha_{mf} d_{mean}}{k_L} = Nu_L \left(4.6/X_{tt}\right) \qquad [11.8.1]$$

where the liquid-phase Nusselt number Nu_L was correlated as

$$Nu_L = 0.045 Re_L^{0.8} Pr_L^{0.4} \qquad [11.8.2]$$

His liquid-phase Reynolds number Re_L is based on the liquid fraction of the flow:

$$Re_L = \dot{m}(1-x) d_{mean} / \mu_L \qquad [11.8.3]$$

The Martinelli parameter for both phases turbulent X_{tt} is

$$X_{tt} = \left(\frac{1-x}{x}\right)^{0.9} \left(\frac{\rho_G}{\rho_L}\right)^{0.5} \left(\frac{\mu_L}{\mu_G}\right)^{0.1} \qquad [11.8.4]$$

In these equations, the maximum internal diameter of the microfin tube was not used. Instead, α_{mf} refers to the local microfin flow boiling coefficient at d_{mean}, which is the mean microfin diameter (that at half the fin height). The correlation for Nu_L was obtained by fitting the Dittus-Boelter correlation to single-phase test data for their one microfin tube, obtaining 0.045 rather than 0.023. Consequently, the method is *not* general but only applicable to that particular microfin tube geometry.

Kido, Taniguchi, Taira and Uehara (1995) measured R-22 heat transfer performances for seven microfin tubes and compared their results to the above method, but found poor agreement. They then proposed another microfin correlation that fit 80% of their data to within ±20% based on their R-22 data. Thus, it must still be compared to other fluids, tube diameters, and microfin geometries to determine if it has general application capabilities. Koyama, Yu, Momoki, Fujii and Honda (1996) ran evaporation tests for R-22, R-134a and R-123 in one microfin tube and proposed a new microfin flow boiling correlation based on these data. However, subcooled liquid test data are required for the particular microfin tube to determine its empirical parameters to correct the Dittus-Boelter correlation, similar to that of Fujii et al. (1993).

Kandlikar and Raykoff (1997) revised an earlier Kandlikar (1991) curvefitting approach for microfin tubes, retaining the fluid specific correction factors from that study, i.e. 1.5 for R-12, 2.2 for R-22, 1.3 for R-113, 1.9 for R-123 and 1.63 for R-134a, similar to the approach in the Kandlikar (1990) plain tube

method. In their approach, each particular microfin geometry requires its own set of three empirical constants to fit the equations to each fluid/tube combination. Subcooled liquid turbulent flow data for each microfin microfin geometry are also required. Hence, this formulation, while interesting, is not amenable to general use.

Thome, Kattan and Favrat (1997) proposed a new microfin flow boiling model, valid for vapor qualities from 0.15 to 0.81, heat fluxes from 2-47 kW/m^2 (630-15000 Btu/h ft^2) and mass velocities from 100-501 kg/m^{2}s (73,581-368,641 lb/hr ft^2), however only verified for R-134a and R-123 data for one microfin geometry. Compared to their ammonia microfin tube data, Kabelac and de Buhr (2001) on the other hand found it to over predicted their data by 30%. The new microfin model includes some of the Thome (1991) model's concepts adapted to the new annular film flow model of Kattan, Thome and Favrat (1998c) for plain tubes. The new microfin flow boiling model incorporates heat transfer augmentation into their asymptotic flow boiling model, where the local microfin flow boiling heat transfer coefficient α_{mf} is determined from the following equation

$$\alpha_{mf} = E_{mf}\left[(\alpha_{nb})^3 + (E_{RB}\alpha_{cb})^3\right]^{1/3} \qquad [11.8.5]$$

α_{nb} is obtained with the Cooper (1984) *dimensional* nucleate pool boiling correlation for pure fluids:

$$\alpha_{nb} = 55 p_r^{0.12}\left(-\log_{10} p_r\right)^{-0.55} M^{-0.5} q^{0.67} \qquad [11.8.6]$$

in which α_{nb} is in W/m^{2}K, p_r is the reduced pressure, M is the molecular weight and q is the local heat flux in W/m^2 determined from the total internal surface area (not the nominal I.D. area). [*Note*: this expression only works in SI units]. Since microfins are small, their fin efficiencies are very close to 100% and this is what was assumed. The convective flow boiling contribution to horizontal flow boiling in a microfin tube ($E_{RB}\,\alpha_{cb}$) is obtained using the turbulent film flow correlation of Kattan, Thome and Favrat (1998c) for plain tubes to calculate α_{cb}. Their convective boiling heat transfer coefficient for the annular film is:

$$\alpha_{cb} = 0.0133\left(Re_L\right)_{film}^{0.69} Pr_L^{0.4}\left(k_L/\delta\right) \qquad [11.8.7]$$

where k_L is the liquid thermal conductivity. The constants 0.0133 and 0.69 are those for the plain tube (not from the present microfin database), which was developed from an experimental database for refrigerants R-123, R-134a, R-502, R-402A and R-404A (since shown to predict R-407C and ammonia flow boiling data without modification). In this expression, the liquid film Reynolds number is determined from the mean velocity of the liquid in the annular film using the local void fraction as:

$$\left(Re_L\right)_{film} = \frac{4\dot{m}(1-x)\delta}{(1-\varepsilon)\mu_L} \qquad [11.8.8]$$

Here, $\dot{m}$ is the total mass velocity of liquid and vapor, ε is the local void fraction and δ is the local thickness of the annular liquid film (ignoring any effect of the microfins) while x is the local vapor quality and μ_L is the liquid dynamic viscosity. The local void fraction is determined using the Rouhani and Axelsson (1970) drift flux model void fraction correlation for plain tubes:

$$\varepsilon = \left(\frac{x}{\rho_L}\right)\left\{\left[1+0.12(1-x)\right]\left(\frac{x}{\rho_G}+\frac{1-x}{\rho_L}\right)+\frac{1.18(1-x)\left[g\sigma(\rho_L-\rho_G)\right]^{0.25}}{\dot{m}^2\rho_L^{0.5}}\right\}^{-1} \qquad [11.8.9]$$

Here, g is gravitational acceleration (9.81 m/s^2) and σ is the surface tension of the fluid (all in SI units). The local annular liquid film thickness is calculated from the cross-sectional area occupied by the liquid phase, assuming uniform thickness of the film around the tube perimeter and ignoring the presence of the microfins, as:

$$\delta = \frac{(1-\varepsilon)d_f}{4} \qquad [11.8.10]$$

The maximum internal diameter at the base of the microfin tube is d_f. The ribbed tube enhancement factor E_{RB} for single-phase turbulent tube flow correlation of Ravigururajan and Bergles (1985) is introduced to include the enhancement effect of the microfins on the convective boiling coefficient:

$$E_{RB} = \left\{1+\left[2.64\mathrm{Re}_{RB}^{0.036}\mathrm{Pr}_L^{-0.024}\left(\frac{e_f}{d_f}\right)^{0.212}\left(\frac{p_f}{d_f}\right)^{-0.21}\left(\frac{\alpha_f}{90^o}\right)^{0.29}\right]^7\right\}^{1/7} \qquad [11.8.11]$$

where e_f is the microfin height (in m), p_f in the axial pitch from fin to fin (in m), α_f is the helix angle of the microfins (in °) and Pr_L is the liquid Prandtl number. Re_{RB} is the liquid-phase tubular Reynolds number defined as

$$\mathrm{Re}_{RB} = \frac{\dot{m}(1-x)d_f}{\mu_L} \qquad [11.8.12]$$

The Grigorig effect enhances film evaporation by drawing the liquid film from the microfin tips towards their roots, similar to film condensation on low finned tubes and corrugated surfaces. Their enhancement factor E_{RB} is for *tubular* flow, not *film* flow. Thus, an addition enhancement factor for microfin tubes, E_{mf}, is included to account for these two effects (the only factor specifically based on the microfin test data themselves) and that of mass velocity:

$$E_{mf} = 1.89(\dot{m}/\dot{m}_{ref})^2 - 3.7(\dot{m}/\dot{m}_{ref}) + 3.02 \qquad [11.8.13]$$

Here, $\dot{m}_{ref}$ is a reference value introduced to non-dimensionalize the expression where $\dot{m}_{ref}$ was set to the maximum value tested, i.e. $\dot{m}_{ref}$ = 500 kg/m^{2}s (367,900 lb/hr ft^2).

Figure 11.13 depicts a comparison of the microfin tube model to R-134a test data at a mass velocity of 200 kg/m^{2}s (147,160 lb/hr ft^2). Notably, the slope of the local heat transfer coefficient vs. vapor quality is correctly captured by the void fraction equation in the model. Figure 11.14 shows the predicted local augmentation ratios averaged over a vapor quality from 0.15-0.85 and plotted as a function of mass velocity for R-134a, showing that the model predicts large enhancement at low mass velocities, which then tends towards the microfin's internal area ratio at high mass velocities, typical of nearly all published experimental results.

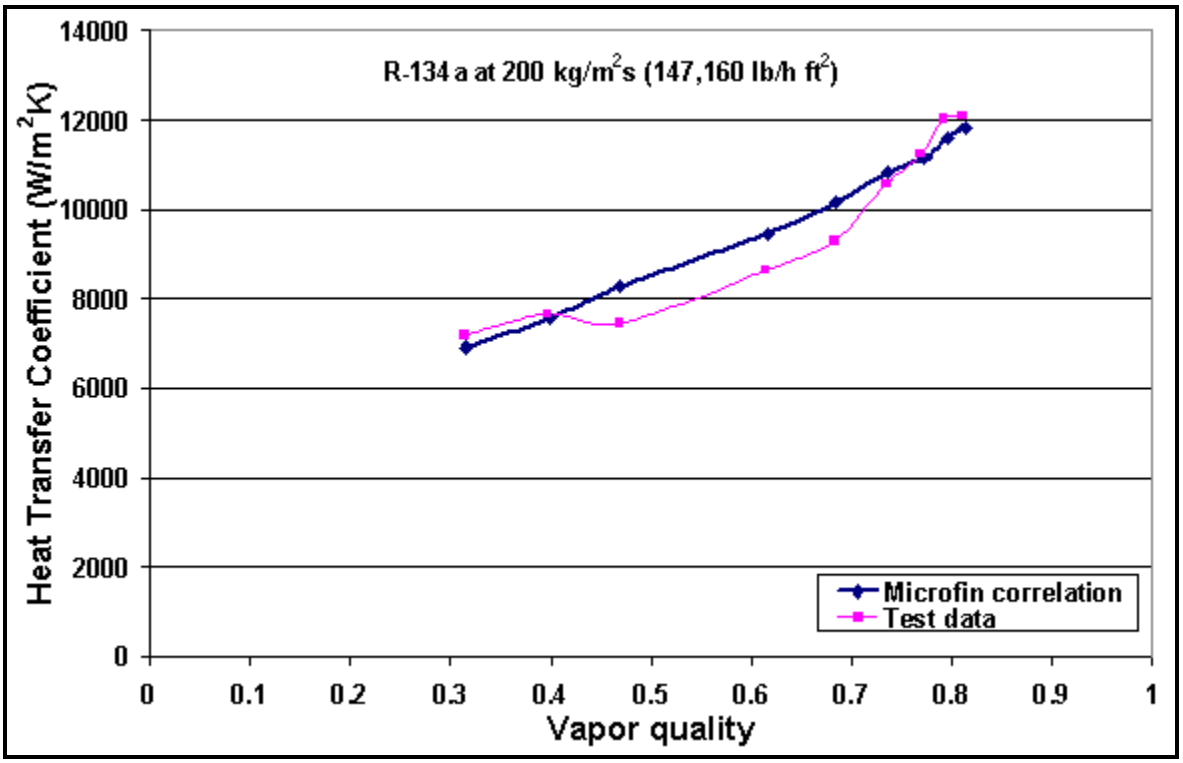

Figure 11.13. Thome, Kattan and Favrat [1997] microfin model compared to R-134a data.

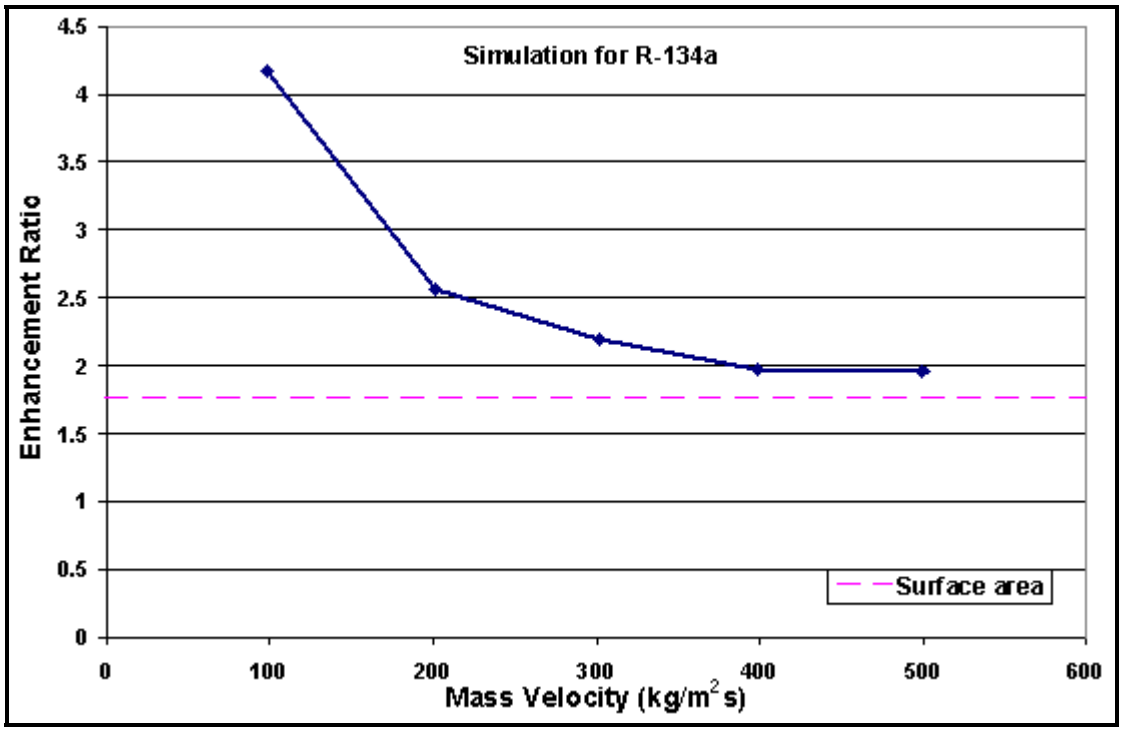

Figure 11.14. Thome, Kattan and Favrat [1997] microfin model showing enhancement ratios as a function of mass velocity.

Since mass velocities in direct-expansion evaporators are normally from about 50 to 500 kg/m^{2}s (36,790 to 367,900 lb/hr ft^2), this expression covers most applications. The value of E_{mf} varies from as high as 2.36 at 100 kg/m^{2}s (73,580 lb/hr ft^2) to as low as 1.21 at 500 kg/m^{2}s (367,900 lb/hr ft^2). A statistical comparison to 362 local heat transfer coefficients gave a standard deviation, a mean deviation and an average deviation for the R-134a data of 18.5%, 12.8% and 2.0%, respectively, while for R-123 the corresponding values were 12.9%, 11.8% and 6.4%. Additional work is required to compare this method to other microfin geometries and fluids. Presently, it covers vapor qualities up to 0.85, which can be assumed to be the point of onset of dryout. For x > 0.85, it is recommended that the heat transfer coefficient be prorated between its value at x = 0.85 and its vapor-phase heat transfer coefficient at x = 1, the latter which is calculated with the Ravigururajan and Bergles (1985) single-phase correlation for ribbed tubes.

In summary, enhancement of microfin flow boiling heat transfer coefficients relative to plain tube values can be attributed to:

- An increase in the convective contribution by the single-phase effect of the microfins;
- A rise in the nucleate boiling contribution by the additional internal surface area;
- Enhancement of annular film evaporation by the Gregorig effect;
- Conversion of stratified-wavy flow (partially wetted tube perimeter) to annular flow (complete wetting) at low mass velocities.

11.9 Correlation for Horizontal Tubes with Twisted Tape Insert

For evaporation inside horizontal tubes with twisted tape inserts, Kedzierski and Kim (1998) proposed a correlation based on experimental data for one twisted tape (Y = 4.15) with five pure fluids and two azeotropes (1401 data points) where Y is the twist ratio. The twist ratio Y is defined as the length along the tube for a 180° turn of the tape divided by the internal tube diameter d_i. Their correlation for the twisted tape flow boiling heat transfer coefficient α_{tt} based on the plain tube internal diameter d_i and reduced pressure p_r is:

$$\frac{\alpha_{tt} d_i}{k_L} = 1.356\, Sw^{c_1}\, Pr_L^{c_2}\, p_r^{c_3} \left(-\log_{10} p_r\right)^{c_4} Bo^{c_5} \qquad [11.9.1]$$

The Swirl number Sw is:

$$Sw = \frac{Re_s}{\sqrt{Y}} \qquad [11.9.2]$$

The swirl Reynolds number Re_s is defined as:

$$Re_s = Re_{Lt} \frac{\sqrt{1+\left(\frac{\pi}{2Y}\right)^2}}{1-\frac{4t}{\pi d_i}} \qquad [11.9.3]$$

where the tape thickness is t. The Reynolds number Re_{Lt} for the total flow as liquid is

$$Re_{Lt} = \frac{\rho_L \dot{m} d_i}{\mu_L} \qquad [11.9.4]$$

Finally, the Boiling number is defined as

$$Bo = \frac{q}{\dot{m} h_{LG}} \qquad [11.9.5]$$

where h_{LG} is the latent heat, q is the local heat flux and $\dot{m}$ is the total mass velocity. The empirical exponents are a function of vapor quality, x:

$$c_1 = 0.993 - 1.181x + 0.899x^2 \qquad [11.9.6]$$

$$c_2 = 1.108 - 2.366x + 1.451x^2 \qquad [11.9.7]$$

$$c_3 = -2.383 + 5.255x - 1.791x^2 \qquad [11.9.8]$$

$$c_4 = -3.195 + 6.668x \qquad [11.9.9]$$

$$c_5 = 1.073 - 2.679x + 1.443x^2 \qquad [11.9.10]$$

Hence, they used 15 empirical constants in their correlation. Other than for statistical expediency, it is not clear why the exponent on the liquid Prandtl number should be a function of vapor quality, ranging from a value of $c_2 = 1.108$ at x = 0 for all liquid flow to only $c_2 = 0.193$ at x = 1 for all vapor. This method did compared well to the data of Agrawal, Varma and Lal (1986) for R-12 at a twist ratio of 5.58. It is thus okay to use but probably its values should be compared to a good plain tube method to see if the enhancement ratio is reasonable or not.